Statistical Geometry of Paper Cross-Sections

K. NISKANEN and H. RAJATORA

We studied paper structure using thin sections of handsheets. The size distribution of z-directional pore spaces (or pore heights) was approximately exponential, demonstrating that the z-directional network structure is essentially random. Measured values for porosity ranged from 0.35–0.5 and for relative bonded area (RBA) from 0.1–0.2. The experimental results are consistent with a simple theory that connects sheet porosity, RBA and pore heights. The predicted relationships depend explicitly on measurement resolution and thickness of dry fibres.

Nous avons étudié la structure du papier à l'aide de minces sections de feuilles d'essai. La répartition en dimension des espaces des pores en direction Z (ou hauteur des pores) était approximativement exponentielle, ce qui indique que la structure du réseau en direction Z est essentiellement aléatoire. Les valeurs de porosité mesurées vont de 0,35 à 0,5, et pour les secteurs liés relatifs, de 0,1 à 0,2. Les résultats des essais correspondent à une théorie simple reliant la porosité de la feuille, le secteur lié relatif, et la hauteur des pores. Les relations prévues dépendent explicitement des résultats des mesures et de l'épaisseur des fibres sèches.

INTRODUCTION

One can characterize the three-dimensional fibre network structure of paper by pore size distributions or mean properties such as sheet porosity and relative bonded area (RBA) of fibres. Although no rigorous relationships have been published, one expects intuitively that pores should be large and RBA low if porosity is high. In this report we will derive the mathermatical relationships and show that they are consistent with experimental observations.

Good overviews of previous knowledge on sheet structure can be found in Refs. [1–3]. The two-dimensional fibre network has been described mathematically by Corte and Kallmes [4]. They found good agreement with data measured on thin two-dimensional sheets. Kallmes et al. [5] also showed how the RBA increases with increasing grammage of the two-dimensional sheet. Dodson and Sampson [6]

JPPS
K. Niskanen and H. Rajatora
KCL Science and Consulting
P.O. Box 70
02151 Espoo, Finland
(kaarlo.niskanen@kcl.fi)

recently extended the analysis to nonrandom sheet structures. No connection between pore diameters and sheet porosity was given.

Corte and Lloyd [7] described the three-dimensional fibre networks by considering random stacks of two-dimensional networks. Pores were characterized by cylinders through which fluids can be thought of penetrating. The calculated hydrodynamic pore diameters were well approximated by a log-normal distribution. Air permeation and oil penetration measurements were consistent with the log-normal distribution [7,8]. Görres et al. [9,10] have continued the work of Corte and Lloyd on multiplanar fibre network models.

Another line of experiments has been the analysis of sheet cross-sections. Yang et al. [11] measured bonding degrees of different paper samples and Paavilainen [12] provided data on the porous network geometry. Szikla and Paulapuro [13] analyzed z-dimensional density distributions from cross-sections. Bonding degrees were also determined using crossed polarizers [14]. Common to these studies is the great amount of microscopy work required. Relationships between pore dimensions and sheet porosity have not been examined with these techniques.

Computer simulations have provided insights into the effect of fibre properties and sheet grammage on the statistical geometry of random fibre networks [15,16]. For example, relationships were reported between the RBA, number of pores and coverage (i.e. number of fibre layers); and between pore dimensions and RBA. No theoretical explanation was given to the numerical results. The practical relevance of the simulation model may be questioned since comparison with experiments was not presented.

In the work with simulated fibre networks, pore geometry was characterized by the free span lengths between fibres in the principal directions of the sheet. The free span lengths did not obey the log-normal distribution that was derived for the hydrodynamic radii by Corte and Lloyd [7]. Instead, the distributions of free span lengths appeared to be exponential (or geometric), just as the length distribution of fibre segments in two dimensions [4]. In this report, we adopt the approach used in the computer simulations to characterize sheet structures with the "pore height" or free span between fibres in the z direction.

In the following, we first present a model that connects pore height with porosity and RBA, and then compare the model predictions with measurements on sheet cross-sections.

THEORY

We consider paper structure along lines through the sheet in the z direction. Such lines can be measured from sheet cross-sections, as will be discussed in the next section. The positions of fibres along such lines define sheet porosity, RBA and the mean height of the interfibre pore space. Our analysis cannot give the properties of separate pores. Instead, it treats the porous space as a whole. This is different from previous studies where the hydrodynamic radii of the individual pores were measured [1,3,5,6,8]. We use the term pore height to indicate that our results differ from the hydrodynamic pore size.

Before going into details, we have to address two general issues that apply to both the theory and experiments. First, we want to redefine porosity ϕ. Usually, porosity is obtained by dividing the total pore volume by the total volume of the sheet. This is equivalent to defining porosity as the ratio of the total height of pores along one typical z-directional line, denoted Σh, and the mean thickness of the sheet. However, that definition corresponds to having always zero porosity at sheet surfaces because there is always a fibre at both ends of the line for local sheet thickness. In reality, porosity is not zero at sheet surfaces because there are holes in the surface. The artifact is avoided when we define porosity relative to sheet thickness minus the thickness of one fibre, t_{fibre}:

$$\phi = \frac{\Sigma h}{\Sigma h + (c-1)\cdot t_{fibre}} \tag{1}$$

where c is coverage, the number of fibres per one scanning line through sheet thickness. This definition means that the reference thickness of the sheet is measured from the middle point of the fibre at the top to the middle point of the fibre at the bottom. It follows that we can calculate porosity from the mean distance $\langle z \rangle$ between the middle points of any two fibres. For example, using adjacent fibres we would obtain

$$\phi = \frac{\langle z \rangle - t_{fibre}}{\langle z \rangle} \tag{2}$$

Equation (2) leads to a connection between pore heights and porosity.

The second point is that any measurement of the sheet structure has a finite resolution. In cross-sectional images, this resolution is determined by the pixel size a. The scanning lines through the sheet are divided into segments of length a and we cannot detect details finer than a. In particular, if the distance between two fibre surfaces is less than a, the fibre surfaces appear to be bonded together. The measurement resolution must have an effect on the values of RBA and therefore cannot be ignored in the analysis. However, we can assume that in any sensible measurement, the pixel size a is much smaller than sheet thickness.

For modeling purposes, we assume that sheet structure is random in the z-direction. This means that when following a z-directional scanning line inside the sheet, fibre positions on the line are random except that fibres cannot intersect. Therefore, each fibre occupies t_{fibre}/a adjacent line segments and any line segment contains at most one fibre. We can now completely specify the structure along a scanning line by giving the locations of the empty line segments. Furthermore, this definition does not change if we remove all but one of the t_{fibre}/a consecutive segments occupied by each fibre. We then have a "renormalized" or "decimated" system. If the original scanning line had N line segments and n fibres, the renormalized line has $N - n\,t_{fibre}/a$ empty and n occupied line segments. In the renormalized system, the line segments occupied by fibres can be selected at random.

Next, we make use of the assumption that the pixel size a is much smaller than sheet thickness. This means that in the renormalized system there are many more empty line segments than occupied line segments. Let $q \approx 1$ be the probability of an empty segment. Then the probability of finding exactly n empty cells (or a pore of height $h = na$) between two fibres is $(1-q)\cdot q^n$. If $n = 0$, there is no pore between the two fibres. Therefore the probablity distribution of pore heights is $(1-q)\cdot q^{n-1}$. Straightforward calculation gives the mean value and standard deviation of pore heights (denoted $\langle h \rangle$ and σ_h).

$$\langle h \rangle = \frac{a}{1-q} \tag{3}$$

and

$$\sigma_h = \frac{\sqrt{q}\,a}{1-q} \tag{4}$$

The total height of pores is the same in the original and renormalized system. From this it follows that

$$q = \left[1 + \frac{1-\phi}{\phi}\,\frac{a}{t_{fibre}}\right]^{-1} \tag{5}$$

and furthermore

$$\langle h \rangle = \frac{\phi}{1-\phi}\,t_{fibre} + a \tag{6}$$

The pixel size a enters in Eq. (6) because the smallest pore height that is counted is equal to a. This introduces the bias a to the mean pore height in Eq. (6). We observe that Eq. (2) implies

$$\langle z \rangle - t_{fibre} = \langle h \rangle - a \tag{7}$$

This verifies that a would be absent from Eq. (6) if we would have included also the pores of zero height in the calculation. Furthermore, we can see that in fact Eq. (6) follows immediately from our definition of porosity.

When a is small ($\ll t_{fibre}$), the standard deviation of pore heights is given by

$$\sigma_h = \langle h \rangle - \frac{1}{2}a \tag{8}$$

Knowing q from Eq. (5), we can also calculate the RBA. If a segment in the renormalized model system contains a fibre then the adjacent segment contains another fibre with probability $1-q$. In a sheet of finite coverage c, there can be at most $c - (1 - \exp(-c))$ interfibre bonds along a z-directional line [5]. Of these, the fraction $1-q$ actually form a bond, or

$$RBA = (1-q)\cdot\left[1 - \frac{1}{c}\left(1-e^{-c}\right)\right] = \frac{a}{\langle h \rangle}\cdot\left[1 - \frac{1}{c}\left(1-e^{-c}\right)\right] \tag{9}$$

We can see that the measurement resolution has a very direct effect on RBA. If

TABLE I
HANDSHEET PROPERTIES

	Kraft, SR13	Kraft, SR25	Kraft, SR35	Kraft, SR45	100% PGW	PGW + 40% kraft	PGW + 40% sulphite	100% kraft	100% sulphite
Grammage (g/m^2)	64.2	63.7	63.3	62.0	60.3	64.8	64.8	63.8	63.4
Apparent density (kg/m^3)	563	657	681	698	447	623	690	725	846
Light scattering coeff. (m^2/kg)	30.2	22.1	21	20.9	79.4	40.4	33.9	16.7	8.12
Tensile index (Nm/g)	23.6	80.9	89.7	92.7	47.4	54.4	53.4	87.5	80.3
Gurley air resistance (s)	1.1	9.7	26	110	N/A	N/A	N/A	N/A	N/A

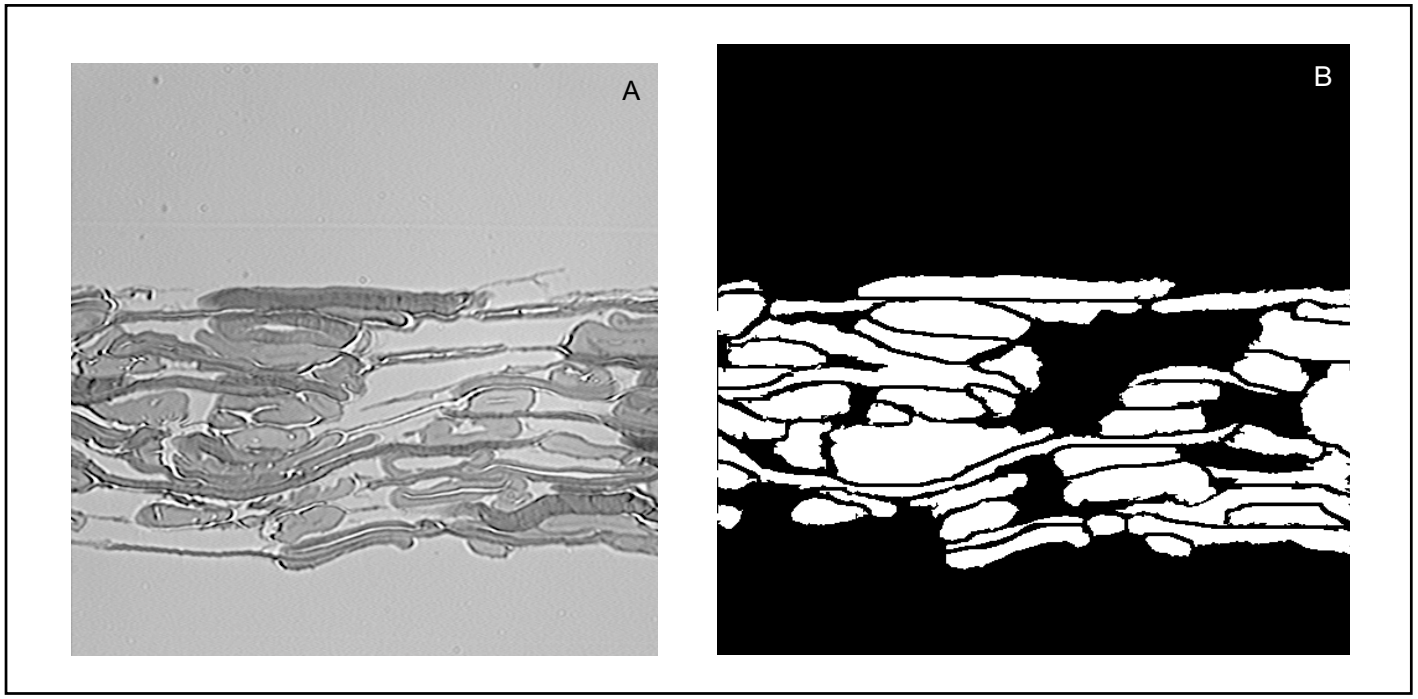

Fig. 1. A) Light microscope image of a cross-section from a pure kraft handsheet. B) The corresponding binary image where all cracks, lumina and fibre wall pores are filled. Image size is 205 μm x 205 μm.

one knows the mean pore height from other sources, then RBA can be calculated for any resolution using the second equality. The prediction relies heavily on the assumption of completely random structure and hence exponential distribution of pore heights. If this is not true at small pore heights, then the calculated RBA is not correct.

EXPERIMENTAL METHODS AND MATERIALS

Two series of handsheet samples were prepared according to SCAN-C26:76 [17]. All pulps were made of Scandinavian softwoods. The first sample set was made of a commercial reinforcement kraft pulp, beaten with a Valley beater to SR values 13, 25, 35 and 45 (CSF 690, 500, 380 and 220 mL, respectively). The second series compared a kraft and sulphite pulp. The pulps were cooked and bleached in laboratory conditions and beaten with a conical disc refiner at 150 kWh/t specific energy consumption. In addition to pure sheets, both pulps of the second series were mixed with 60% of a commercial lightweight coated grade pressurized groundwood (PGW). Pure PGW handsheets were also evaluated. Some standard properties of the paper samples are given in Table I.

The cross-section analysis started with stained thin sections viewed under a light microscope. Prior to epoxy embedding, the samples were stained with methyl blue. The sections were 3 μm thick. A low-pass filtered binary image (pixel size 0.4 μm) was formed to separate fibrous material from the epoxy. Next, lines were drawn manually to separate bonded fibre surfaces. The original micrograph was used as a reference when choosing the bonded interfaces. The lines added at bonded interfaces were in practice 1.2 μm thick. This means that even pores that were less than 1.2 μm thick were manually broadened to the minimum thickness of 1.2 μm. Once the fibres were separated, all lumen spaces and cell wall cracks in the images could be filled automatically. Thus, the final binary image revealed the pore space between fibres while pore spaces encircled by a fibre wall were regarded as part of the fibre. Figure 1 illustrates the image analysis procedure.

The pore structure was measured by scanning along lines in the z direction through the binary images. Each image was 205 μm wide. Eighty lines per image were scanned. The number of binary images ranged from 15–50 per sample so that at least 1200 lines per sample were scanned. From the binary images, we determined the distribution of pore heights and fibre thicknesses. The pore height distributions were reasonably close to the theoretical exponential shape, as illustrated in Fig. 2. The measured distributions start from the 1.2 μm bin because the manual image editing broadened all thinner pores to this minimum thickness. Apparently the manually added bond lines did not contribute much to the 1.2 μm bin in the height distribution. Fibre thicknesses obeyed the normal distribution.

We also determined porosity ϕ according to Eq. (1), coverage c and effective density ρ_{eff} of paper from the cross-sectional images. The division of paper grammage by coverage gives fibre grammage β_{fibre}. We then determined effective density from

$$\rho_{eff} = \frac{b - \beta_{fibre}}{t - t_{fibre}} \qquad (10)$$

where b is paper grammage and t is paper thickness, the latter measured from the cross-sectional images. This definition of effective density is consistent with that of porosity in Eq. (1). The effective density according to Eq. (10) avoids the usual ambiguity that one has when

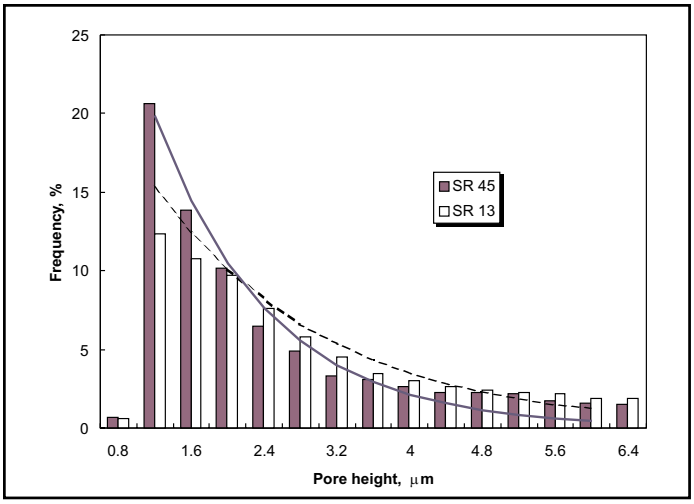

Fig. 2. Height distribution of pore space for the samples SR13 (white bars and dashed line) and SR45 (black bars and solid line). Bin size is 0.4 μm. The bars give measured values and curves give the theoretical result $(1 - q) \cdot q^{h/a-1}$ where q is given by Eq. (5).

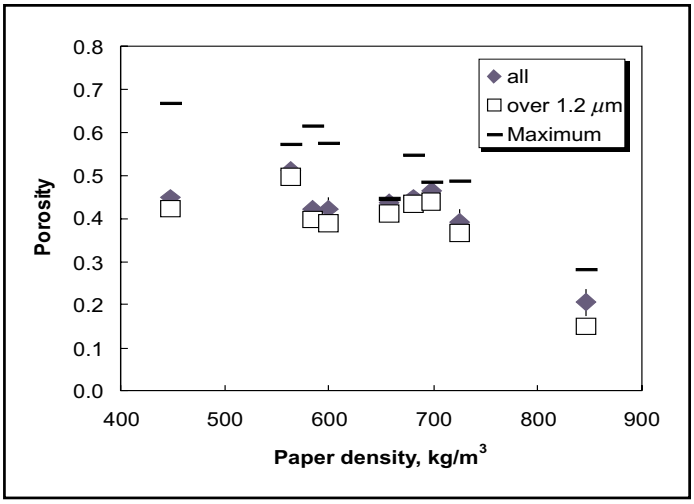

Fig. 3. Porosity against apparent paper density. The flat bars indicate the theoretical maximum value, ϕ_{max}, (Eq. 11), black diamonds the ordinary porosity ϕ that includes all detected pores, and open squares a lower bound value that excludes all pores not more than 1.2 μm high. The error bars show the 95% confidence limits of ϕ.

dealing with surface roughness [18].

The measured values of porosity contain the manually added bonding lines but excludes all intrafibre pores. To determine RBA, pores of thickness 1.2 μm were counted as interfibre bonds, and RBA is given by the number of bonds per scanning line divided by coverage.

The cross-sectional analysis was sensitive to the quality of the cross-sections. For example, parts of fibre wall could easily be counted as lumen when staining was light. Damage inflicted in thin sectioning would also give misrepresentation of the network geometry. A number of images were checked for each sample in an effort to ensure that the measurement was faithful. Yet one can easily spot places in Fig. 1 where the separation of bonded fibres is ambiguous. The finite 3 μm thickness of the sections may also cause smearing of details of the images.

EXPERIMENTAL RESULTS

The sheet parameters obtained from the cross-sectional analysis are shown in Table II. Most values of effective density were 10–20% higher than the corresponding apparent densities (Table I). The difference in apparent density was similar to that obtained with other methods, such as the rubber platen and mercury immersion techniques [18]. Both the effective density and apparent density changed systematically when mixing PGW and chemical pulps. In the beating set, the effective density values varied irregularly. Damage inflicted in sectioning or imperfect staining are the most probable causes for the variability. It is reasonable to assume that effective density increases in beating at the same relative rate as does apparent density.

Except for the 100% sulphite pulp, porosity in the handsheets was between 0.4 and 0.5, although the apparent density of paper varied almost by a factor of two, from 450–850 kg/m^3 (Fig. 3). Of the three porosity values for each handsheet that are shown in Fig. 3, the lowest one includes only pores that are at least 1.2 μm thick and the next largest one contains all pores visible in the binary cross-section images. The sheet porosities ϕ given in Table II include all the visible pores. The small difference between the two estimates of porosity demonstrates that the manually added lines at bonded fibre interfaces had only a small effect on porosity. The short lines in Fig. 3 give the maximum value of porosity calculated from the effective density of paper, when assuming that the fibre wall material has the density of 1550 kg/m^3 appropriate for cellulose, or

$$\phi_{\max} = 1 - \rho_{eff} / \left(1550 \text{ kg / m}^3\right) \qquad (11)$$

In some preliminary measurements, we obtained porosity values above the theoretical maximum of Eq. (11). These appeared to be

TABLE II
RESULTS FROM THE CROSS-SECTIONAL ANALYSIS

	Kraft, SR13	Kraft, SR25	Kraft, SR35	Kraft, SR45	100% PGW	PGW + 40% kraft	PGW + 40% sulphite	100% kraft	100% sulphite
Effective density, kg/m^3	662 (12)	860 (25)	701 (17)	800 (20)	517 (13)	599 (19)	660 (18)	796 (26)	1114 (54)
Porosity	0.51 (0.01)	0.44 (0.01)	0.45 (0.01)	0.47 (0.01)	0.45 (0.02)	0.42 (0.02)	0.42 (0.02)	0.39 (0.03)	0.21 (0.03)
Coverage	8.4 (0.33)	7.3 (0.25)	9.0 (0.36)	7.4 (0.30)	13.9 (0.81)	11.9 (0.81)	11.8 (0.80)	7.9 (0.49)	6.6 (0.65)
RBA	0.13 (0.002)	0.17 (0.003)	0.10 (0.006)	0.18 (0.006)	0.16 (0.011)	0.16 (0.008)	0.18 (0.012)	0.18 (0.015)	0.33 (0.019)
Mean pore height, μm	6.0 (0.2)	4.5 (0.2)	4.6 (0.2)	4.9 (0.2)	3.9 (0.2)	4.1 (0.3)	3.6 (0.2)	4.5 (0.5)	2.6 (0.4)
St. dev. of pore height, μm	6.6	4.9	4.5	5.7	3.6	3.9	3.3	5.1	2.6
Fibre thickness, μm	5.6 (0.2)	5.7 (0.2)	5.6 (0.2)	5.7 (0.2)	4.5 (0.3)	5.2 (0.4)	4.8 (0.3)	5.7 (0.4)	6.1 (0.6)

The numbers in parenthesis give the 95% confidence limits, calculated from the variance between cross-sectional images. Effective density was determined according to Eq. (10) and porosity according to Eq. (1)

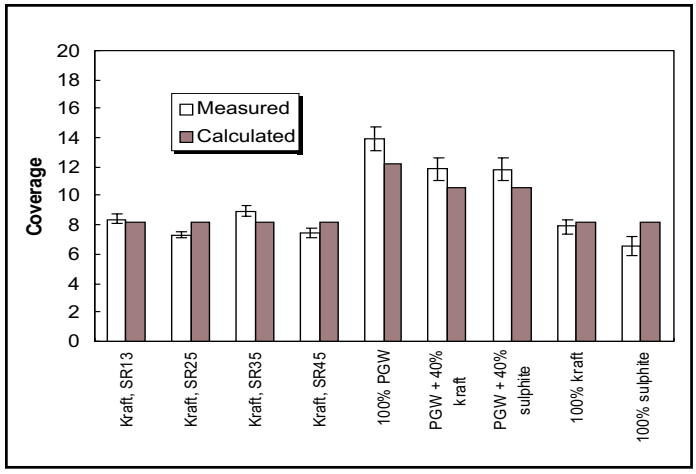

Fig. 4. Coverage values directly measured from cross-sections (white bars) and calculated from $c = b/\beta_{fibre}$ (black bars), where b is paper grammage and $\beta_{fibre} = \rho_{fibre} t_{fibre}$ arises from the apparent fibre density (Eq. 12) and mean fibre thickness t_{fibre} (Table II).

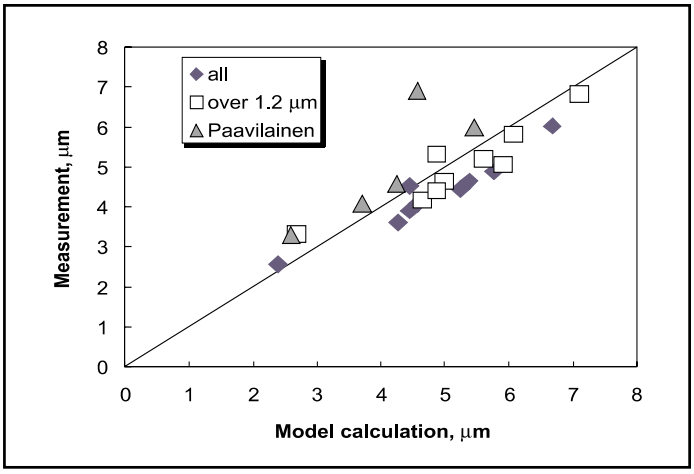

Fig. 5. Comparison of measured and calculated (Eq. 6) values of the mean pore height <h>. All pores included (a = 1.2 μm), and only pore space higher than 1.2 μm included, or a = 1.6 μm (black diamonds and open squares, respectively). Triangles were obtained from the study of Paavilainen [12]. In this case, the corresponding model calculation (Eq. 6) used a = 1.5 μm.

cases where fibre staining was not sufficiently strong. Some of the fibre wall material was then missed when forming the binary image. The fact that the porosities reported here do not exceed the theoretical maximum does not guarantee that no fibre material was missed in these cases.

Unlike the directly measured porosity values, the calculated maximum porosity follows, quite systematically, changes in the apparent density. This suggests that the differences in paper density arise from differences in lumen collapse, as previously concluded by Paavilainen [12]. In our analysis, lumen volume is counted as part of the fibre volume. The volume fraction of lumina therefore contributes to the difference between the calculated maximum porosity and the measured porosity. Additional contributions may arise from artifacts in the analysis of the cross-sectional images.

The apparent fibre density, including lumen space in the fibre volume, is given by

$$\rho_{fibre} = \frac{\rho_{eff}}{1-\phi} \qquad (12)$$

We found no systematic variation in the apparent fibre density of the pure chemical pulp with beating degree or pulp type. The calculated mean value is $\rho_{fibre} \approx 1400$ kg/m^3 for the chemical pulps and $\rho_{fibre} = 940$ kg/m^3 for the PGW. In the mixture sheets, the apparent fibre density agrees with the weighted mean value of PGW and each of the two chemical pulps. The proper value for the mean density is obtained when the weighted mean value is first calculated for bulk and then inverted.

When the apparent fibre density is multiplied by fibre thickness, we obtain fibre grammage β_{fibre}. This in turn allows us to calculate coverage from $c = b/\beta_{fibre}$ where b is paper grammage. We used the mean densities $\rho_{fibre} \approx 1400$ and 940 kg/m^3, and the mean thickness $t_{fibre} = 5.4$ μm of the fibres (differences between kraft and PGW fibre thicknesses were insignificant, see Table II). This gave $\beta_{fibre} = 7.7$ and 5.1 g/m^2 for the kraft and PGW fibres, respectively. The calculated coverage values are consistent with the directly measured values (Fig. 4). The agreement demonstrates that coverage can be calculated if the grammage of dry fibres is known from other sources.

From Table II, one can see that in almost all cases the standard deviation of pore height σ_h and mean pore height $\langle h \rangle$ are equal within the measurement accuracy. This is qualitatively consistent with the theory; according to Eq. (8) the standard deviation should be equal to the mean value minus a/2. Even the calculated pore height distributions, $g(h) = (1 - q) \cdot q^{h/a}$, agree quite well with the experiments, as indicated in Fig. 2. The parameter q follows from Eq. (5), using a = 1.2 μm because smaller pores were erased in the cross-sectional image analysis.

Figure 5 shows that the model calculation gives quite accurate values for the mean pore height $\langle h \rangle$. When the measured sheet porosity ϕ, fibre thickness t_{fibre} (Table II), and the value a = 1.2 μm are inserted in Eq. (6), the result is almost equal to the measured value. The agreement between theory and experiment remains unchanged if also the 1.2 μm bin is excluded. In this case, we also have to re-evaluate the mean pore height.

Paavilainen [12] has reported values for $\langle h \rangle$ from cross-sectional images. These values are somewhat larger than our model, Eq. (6), predicts (see the triangles in Fig. 5). To show this, we calculated porosity from her values of fibre thickness, coverage, mean pore thickness (height) and pore number per scan line. The measurement resolution (cut off) a was not explicitly stated in the report [12], but from the information given a = 1.5 μm seemed reasonable. We selected this value for a since it gave the best agreement with the theory. One of Paavilainen's data points was excluded from Fig. 5 because it fell far from the other points; the measured pore height was 22 μm and calculated 11 μm.

The evaluation of RBA from the cross-sectional images gave only small differences between the samples. The highest value, RBA = 0.33 was obtained for the 100% sulphite pulp. In all the other samples, including 100% PGW, RBA was between 0.1 and 0.2.

Our values for RBA are smaller than those reported by Yang et al. [11]. They found RBA = 0.25 for a newprint made of TMP and RBA = 0.3–0.5 for sheets made from various

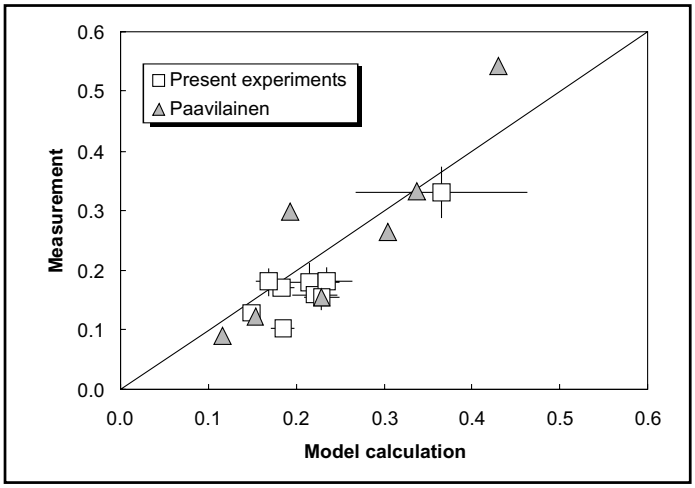

Fig. 6. Measured RBA vs the value given by Eq. (9). The calculated value employs a = 1.6 μm, and the measured values of porosity coverage c (Table II). Error bars indicate 95% confidence intervals. Triangles were obtained from the study of Paavilainen [12] and the corresponding model calculation used a = 1.5 μm.

kraft pulps. The apparent sheet densities were 500 and 630–700 kg/m^3, respectively, suggesting that the interfibre porosities of their samples were similar to ours. RBA and porosity were also obtained from the cross-section study of Paavilanen [12] on kraft handsheets. Please note that Paavilainen reported $RBA + 1/c$, which we converted to RBA using the coverage values given by her. We also calculated porosity from her values of fibre thickness, coverage, mean pore thickness (height) and pore number per scanning line. The resulting RBA values are somewhat higher than those we measured for similar porosities. We believe that the difference arises from the larger pixel size in Paavilainen's study compared to ours, as we will explain later. The same explanation may apply to the results of Yang et al. [11]. Using polarized light on paper surfaces, Page et al. [14] found that RBA increased from 0.16 to 0.36 with beating of a sulphite pulp, which is consistent with our findings.

The measured values of RBA can also be compared with the theory, Eq. (9). Since all pores equal to or less than 1.2 μm in height were counted as interfibre bonds, we used a = 1.2 μm in Eq. (11). The best agreement with experiments was obtained when we counted the parameter q from Eq. (5), using the measured porosity, and inserted the result in Eq. (9) (see Fig. 6). If we used the measured mean pore height $\langle h \rangle$ from Table II, the calculated values of RBA would increase on the average by 0.04. In this latter estimate we should recalculate $\langle h \rangle$ so that the pores of height equal to or less than 1.2 mm would not be counted in the mean pore height. However, the effect is insignificant compared to the accuracy of the estimate. The error bars in Fig. 6 were calculated from the variance of measured porosity and coverage, given in Table II.

The RBAs measured by Paavilainen [12] are in rough agreement with our theory (triangles in Fig. 6). In the model calculation we used the value a = 1.5 μm indicated above, the fibre thickness values measured by Paavilainen and the porosity calculated from her data (as explained above).

Our model is also consistent with computer simulations for high-coverage random fibre networks [16]. Bins equal to fibre thickness were employed in the simulations. The result was $RBA = t_{fibre}/\langle h \rangle$ for $c >> 1$. This is equivalent to Eq. (9). The simulated pore heights followed exponential distribution just as we found here.

DISCUSSION

We have demonstrated that the porous network structure of paper is consistent with the assumption that fibres are randomly positioned in the thickness direction of the sheet. This assumption leads to an exponential (or geometric) distribution of pore heights, as is observed both in the present experiments and in previously published computer simulations [16].

On closer examination, both the experiments and simulations show slight deviations from the exponential pore height distribution. There are several mechanisms that can contribute to this. Fibre interactions during sheet consolidation and drying can make the real sheet structure nonrandom. For example, during drying, Campbell forces may reduce the proportion of shallow interfibre pore space. The cross-sectional shape of fibres should also influence the small-pore end of the distribution.

Another factor is the finite thickness of ordinary paper sheets. Computer simulations [16] demonstrate that a minimum coverage must be exceeded before any pores (other than pinholes) can form in the sheet. The minimum coverage is low if fibres are proportionately stiff, and high if fibres are flexible. The cross-over from zero porosity to finite porosities occurs at ordinary paper grammages.

The theoretical model we derived makes use of the assumption of random network structure. The model couples together sheet porosity, fibre thickness and RBA. Its predictions agree quite well with the values we measured, and with those reported by Paavilainen [12]. Even the shape of the measured pore height distribution is fairly well reproduced from the model, using measured porosity and fibre thickness.

The model Eqs. (6) and (9) allow one to estimate RBA from sheet cross-section data ($\langle h \rangle$ and ϕ), without the need to separate bonded fibres manually. It is important to remember that any measurement of RBA relies on a threshold separation below which two fibre surfaces are considered bonded together. In optical measurements, such as those of Page et al. [14], the wavelength of light defines the threshold. This threshold level is similar to the 0.4 μm pixel size in our images. Thus direct measurements of the pore height distribution, without any manual editing of interfibre surfaces, should yield estimates for RBA that compare favourably with other measurements. Such model calculations are naturally accurate only if the random structure assumption is sufficiently close to reality. Particularly thin pore heights may deviate from the exponential distribution so much that the theoretical calculation of RBA becomes unreliable.

ACKNOWLEDGEMENTS

We thank the Technology Development Centre (TEKES) for financial support, Ms. Terttu Wolin, Mr. Vesa Humppi and Mr. Eino Grönlund for performing most of the experiments and Drs. Mikko Alava, Jukka Ketoja and Kari Niemi for fruitful comments.

REFERENCES

1. CORTE, H., "The Structure of Paper" in Handbook of Paper Science, H.F. Rance, Ed., Elsevier, Amsterdam, 2(9) (1982).
2. CORTE, H., "The Porosity of Paper" in Handbook of Paper Science, H.F. Rance, Ed., Elsevier, Amsterdam, 2(6) (1982).
3. DENG, M. and DODSON, C.T.J., Paper – An Engineered Stochastic Structure, TAPPI PRESS (1994).
4. CORTE, H. and KALLMES, O.J., "The Structure of Paper. I. The Statistical Geometry of Ideal Two-Dimensional Fiber Networks", *Tappi* 43(9):737–752 (1960).
5. KALLMES, O.J., CORTE, H. and BERNIER, G., "The Structure of Paper, V. The Bonding States of Fibres in Randomly Formed Paper", *Tappi J.* 46(8):493–502 (1963).
6. DODSON, C.T. J. and SAMPSON, W.W., "The Effect of Paper Formation and Grammage on its Pore Size Distribution", *J. Pulp Paper Sci.* 22(5):165–169 (1996).
7. CORTE, H.K. and LLOYD, E.H., "Fluid Flow Through Paper and Sheet Structure" in Consolidation of the Paper Web, F. Bolam, Ed., B.P.M.A., London, 981–1009 (1966).
8. BLEISNER, W.C., "A Study of the Porous Structure of Fibrous Sheets Using Permeability Techniques", *Tappi J.* 47(7):392–400 (1964).
9. GÖRRES, J., SINCLAIR, C.S., and TALLENTIRE, A., "An Interactive Multiplanar Model of Paper Structure", *Paperi ja Puu* 71(1):54-59 (1989).
10. GÖRRES, J.F., AMIRI, R. and McDONALD, D., "The Specific Pore Volume of Multi-Planar Webs: The Role of the Short and Long Fibre Fractions" in The Science of Papermaking, C.F. Baker, Ed., The Pulp and Paper Fund. Res. Soc., Bury, 1371–1383 (2001).
11. YANG, C.F., EUSUFZAI, A.R.K., SANKAR, R., MARK, R.E. and PERKINS, R.W., "Measurements of Geometric Parameters of Fibre Networks. Part 1. Bonded Surfaces, Aspect Ratios, Fibre Moments of Inertia, Bonding Site Probabilities", *Svensk Papperstidn.* 81(13): 426–433 (1978).
12. PAAVILAINEN, L., "Bonding Potential of Softwood Sulphate Fibres", *Paperi ja Puu* 76(3):162–173 (1994).
13. SZIKLA, Z. and PAULAPURO, H., "Changes in z-Direction Density Distribution of Paper in Wet Pressing", *J. Pulp Paper Sci.* 15(1):J11–J17 (1989).
14. PAGE, D.H., TYDEMAN, P.A. and HUNT, M., "A Study of Fibre-Fibre Bonding by Direct Obervation" in The Formation and Structure of Paper, F. Bolam, Ed., B.P.B.M.A., London, 171–193 (1961).
15. NISKANEN, K., NILSEN, N., HELLÉN, E. and ALAVA, M., "KCL-PAKKA, Simulation of the 3D Structure of Paper" in The Fundamentals of Papermaking Materials, Pira Intl., Leatherhead 1273–1291 (1997).
16. HELLÉN, E.K.O., ALAVA, M.J. and NISKANEN, K.J., "Porous Structure of Thick Fibre Webs", *J. Appl. Phys.* 81(9):6425–6431 (1997).
17. "Pulp – Preparation of Laboratory Sheets for Physical Testing", Test Method SCAN-C 26:76, Scandinavian Pulp, Paper and Board Testing Comm. (1975).
18. WINK, W.A. and BAUM, G.A., "A Rubber Platen Caliper Gauge – A New Concept in Measuring Paper Thickness", *Tappi J.* 66(9): 131–133 (1983).

REFERENCE: NISKANEN, K. and RAJATORA, H., Statistical Geometry of Paper Cross-Sections, Journal of Pulp and Paper Science, 28(7):228–233 July 2002. Paper offered as a contribution to the Journal of Pulp and Paper Science. Not to be reproduced without permission from the Pulp and Paper Technical Association of Canada. Manuscript received April 18, 2001; revised manuscript approved for publication by the Review Panel February 4, 2002.

KEYWORDS: CROSS SECTION, HAND SHEETS, PAPER STRUCTURE, PORES, DIMENSIONS, Z DIRECTION, NETWORKS, POROSITY, GEOMETRY.